

Phase Transitions in the NMSSM

Koichi Funakubo^{a,1}, Shuichiro Tao^{b,2} and Fumihiko Toyoda^{c,3}

^{a)}Department of Physics, Saga University, Saga 840-8502 Japan

^{b)}Department of Physics, Kyushu University, Fukuoka 812-8581 Japan

*^{c)}School of Humanity-Oriented Science and Engineering, Kinki University, Iizuka
820-8555 Japan*

Abstract

We study phase transitions in the Next-to-Minimal Supersymmetric Standard Model (NMSSM) with the weak scale vacuum expectation values of the singlet scalar, constrained by Higgs spectrum and vacuum stability. We find four different types of phase transitions, three of which have two-stage nature. In particular, one of the two-stage transitions admits strongly first order electroweak phase transition, even with heavy squarks. We introduce a tree-level explicit CP violation in the Higgs sector, which does not affect the neutron electric dipole moment. In contrast to the MSSM with the CP violation in the squark sector, a strongly first order phase transition is not so weakened by this CP violation.

¹e-mail: funakubo@cc.saga-u.ac.jp

²e-mail: tao@higgs.phys.kyushu-u.ac.jp

³e-mail: ftoyoda@fuk.kindai.ac.jp

1 Introduction

The origin of matter has been a long standing problem in astrophysics and particle physics. Several attempts have been made to explain how the matter-antimatter asymmetry was generated starting from the symmetric universe, in the early stage of the universe before the nucleosynthesis. Among such attempts, electroweak baryogenesis is a scenario which is intimately related to physics at our reach[1]. The scenario of electroweak baryogenesis, however, requires extension of the minimal standard model, since the minimal standard model with the Higgs boson heavier than the present bound does not give rise to strongly first-order phase transition, which is required to realize nonequilibrium state, and CP violation in the CKM matrix is too small to generate sufficient baryon number. Hence one needs extra sources of CP violation and light bosons, which strengthen the electroweak phase transition (EWPT). The minimal supersymmetric standard model (MSSM) is one of such extensions of the standard model, which can provide strongly first-order EWPT and contains many sources of CP violation. The first-order EWPT is expected in the MSSM with a light top squark ($m_{\tilde{t}_1} \leq m_t$), which enhances v^3 -behavior of the effective potential, where v represents the expectation value of the Higgs fields. The behavior is also enhanced for smaller $\tan \beta$, that is, larger top Yukawa coupling. The present bound on the lightest Higgs boson restricts the acceptable parameter space of the model, which incorporates the strongly first-order EWPT. Further, the first-order EWPT is weakened, when the stop sector CP violation, characterized by $\text{Im}(\mu A_t e^{i\theta})$, is large, where θ is the relative phase of the two Higgs doublets[2]. Thus, we are left with rather restricted range of the parameter region available for the baryogenesis in the MSSM.

Another extension of the standard model is the next-to-minimal supersymmetric standard model (NMSSM), which contains an extra singlet chiral superfield. It shares the advantages of the MSSM and solves the μ -problem inherent in the MSSM. The NMSSM is reduced to the MSSM in the limit where the singlet decouples leaving a finite μ -term. For such peculiar parameters, we expect the same behavior of the EWPT as that in the MSSM, which has been extensively studied. Here we shall focus on the parameter space far from the MSSM, that is, the case where the vacuum expectation value of the singlet scalar has the magnitude of the weak scale. One naturally expects such parameters, when all the soft masses of the scalars are generated at the same scale where the supersymmetry is broken. For such parameters, two of the authors studied Higgs spectrum with and without CP violation. In [2], two distinct allowed parameter regions are chosen after imposing conditions for the model to yield the sensible electroweak-breaking vacuum. The lightest Higgs boson for one type of the allowed parameter sets has moderate coupling to Z boson, while its mass is heavier than 114GeV. The other type of the parameter sets contains the Higgs bosons lighter than the bound, but their couplings to the Z boson are too small to be produced in the e^-e^+ colliders. For such parameters, only the Higgs boson heavier than the bound has the chance to be observed in future collider experiments.

Our purpose is to study finite-temperature phase transitions in the NMSSM with and

without CP violation in the Higgs sector. We find that the transitions in the case with light Higgs bosons are very different from that in the others. This paper is organized as follows. In Section 2, we introduce the model and define the parameters in the Higgs potential in a manner independent of the phase conventions. The effective potential including at the one-loop level is given in Section 3. Based on the symmetry of the effective potential, we discuss the possible phases and transitions among them in Section 4. In Section 5, we present the numerical results on the phase transitions with and without the explicit CP violation in the Higgs sector. Section 6 is devoted to discussions on our results and their implication on the baryogenesis. We summarize some formulas to calculate the effective potential in Appendix.

2 The model

The NMSSM is an extension of the MSSM, which contains one singlet superfield N . The superpotential of the model is

$$W = \epsilon_{ij} \left(y_b H_d^i Q^j B - y_t H_u^i Q^j T + y_l H_d^i L^j E - \lambda N H_d^i H_u^j \right) - \frac{\kappa}{3} N^3, \quad (2.1)$$

which contains no dimensional parameter. The μ -parameter in the MSSM is induced when the scalar component of the singlet N acquires nonzero vacuum expectation value, $\mu = \lambda \langle N \rangle$. We shall not specify how the supersymmetry is broken, so that we introduce generic type of soft supersymmetry-breaking terms. The dimensional parameters such as the scalar masses, A -terms and gaugino masses, are considered as inputs, which are constrained, for example, by vacuum stability conditions. The soft supersymmetry-breaking terms are composed of those in the MSSM with $\mu = 0$ and the terms including the singlet fields:

$$\mathcal{L}_{\text{soft}} = \mathcal{L}_{\text{soft}}^{\text{MSSM}, \mu=0} - m_N^2 n^* n + \left[\lambda A_\lambda n H_d H_u + \frac{\kappa}{3} A_\kappa n^3 + m'_N n^2 + \text{h.c.} \right]. \quad (2.2)$$

Among these terms the n^2 -term breaks the global Z_3 symmetry, which causes the domain wall problem upon broken spontaneously. The n^2 -term is not generated in the simple supergravity model, so we shall not include it in the following and consider that the discrete symmetry is explicitly broken by some higher dimensional operator at very early era before the EWPT.

We parameterize the expectation values of the Higgs scalars as

$$\langle \Phi_d \rangle = \begin{pmatrix} \frac{1}{\sqrt{2}} v_d \\ 0 \end{pmatrix}, \quad \langle \Phi_u \rangle = e^{i\theta} \begin{pmatrix} 0 \\ \frac{1}{\sqrt{2}} v_u \end{pmatrix}, \quad \langle n \rangle = \frac{1}{\sqrt{2}} e^{i\varphi} v_n, \quad (2.3)$$

where Φ_d , Φ_u and n are the scalar components of H_d , H_u and N , respectively.

The tree-level Higgs potential is written as a function of these expectation values:

$$V_0 = \frac{1}{2} m_1^2 v_d^2 + \frac{1}{2} m_2^2 v_u^2 + \frac{1}{2} m_N^2 v_n^2 - \left[\frac{\lambda A_\lambda}{2\sqrt{2}} e^{i(\theta+\varphi)} v_d v_u v_n + \frac{\kappa A_\kappa}{6\sqrt{2}} e^{3i\varphi} v_n^3 + \text{h.c.} \right]$$

$$+\frac{g_2^2+g_1^2}{32}(v_d^2-v_u^2)^2+\frac{|\lambda|^2}{4}(v_d^2+v_u^2)v_n^2+\left|\frac{\lambda}{2}e^{i\theta}v_dv_u+\frac{\kappa}{2}e^{2i\varphi}v_n^2\right|^2, \quad (2.4)$$

where the terms in the first line consist of the soft-supersymmetry breaking terms, while those in the second line come from the D - and F -terms. Here we have four complex parameters λ , κ , A_λ and A_κ , and two phases θ_0 and φ_0 , which are the values of θ and φ evaluated at zero-temperature vacuum. Some of these are redundant, so that we introduce the following notations in order to present the results in a manner independent of phase conventions,

$$R_\lambda = \frac{1}{\sqrt{2}}\text{Re}\left(\lambda A_\lambda e^{i(\theta_0+\varphi_0)}\right), \quad I_\lambda = \frac{1}{\sqrt{2}}\text{Im}\left(\lambda A_\lambda e^{i(\theta_0+\varphi_0)}\right), \quad (2.5)$$

$$R_\kappa = \frac{1}{\sqrt{2}}\text{Re}\left(\kappa A_\kappa e^{3i\varphi_0}\right), \quad I_\kappa = \frac{1}{\sqrt{2}}\text{Im}\left(\kappa A_\kappa e^{3i\varphi_0}\right), \quad (2.6)$$

$$\mathcal{R} = \text{Re}\left(\lambda\kappa^* e^{i(\theta_0-2\varphi_0)}\right), \quad \mathcal{I} = \text{Im}\left(\lambda\kappa^* e^{i(\theta_0-2\varphi_0)}\right). \quad (2.7)$$

As shown in [2], these parameters are constrained by the tadpole conditions, which require the first derivatives of the potential to vanish at the prescribed vacuum. In particular, CP-violation is characterized only by \mathcal{I} , since the conditions lead to

$$I_\lambda = \frac{1}{2}\mathcal{I}v_{0n}, \quad I_\kappa = -\frac{3}{2}\mathcal{I}\frac{v_{0d}v_{0u}}{v_{0n}} = -\frac{3}{2}\mathcal{I}\frac{v_0^2}{v_{0n}}\sin\beta_0\cos\beta_0, \quad (2.8)$$

where the subscripts 0 denote the values evaluated at the vacuum and $\tan\beta_0 = v_{0u}/v_{0d}$. When all the parameters are real, these equations are reduced to a trivial one. If some of them are complex, we must arrange the parameters to respect this condition. In practice, we give the absolute values of the parameters as inputs, then choose their phases so as to satisfy this condition. As for the CP-even parameters, R_λ , R_κ and \mathcal{R} are related to the soft masses. In favor of these parameters, one can eliminate m_1^2 , m_2^2 and m_N^2 in terms of v_0 , v_{0n} and $\tan\beta_0$ by use of the tadpole conditions.

The MSSM limit, for which the singlet scalar decouples by taking $v_n \rightarrow \infty$ with λv_n and κv_n fixed, the model is reduced to the MSSM, in the sense that not only the spectrum but also the behavior of the EWPT are the same as those in the MSSM. In the following, we focus on the case of weak scale v_{0n} , for which we expect new features in the Higgs spectrum and the EWPT. Then we obtain some new constraints on the parameters in the model. In the MSSM, the vacuum parameterized by v_0 and $\tan\beta_0$ is the global minimum of the potential, as long as the tadpole conditions are satisfied. On the contrary, in the NMSSM, we must require that the prescribed vacuum is the global minimum of the potential, and masses squared of the other scalars, such as the charged scalars, evaluated there are positive. We also impose the condition that the lightest neutral Higgs mass is heavier than 114GeV when its coupling to the Z boson is not small. These requirements select some allowed parameter sets from the vast parameter space. The allowed parameter sets are classified into two kinds. The one contains a light Higgs boson whose mass is

smaller than 114GeV and the coupling to Z boson is very small. The other consists of the Higgs bosons, all of which are heavier than the bound. We refer to a scenario with the former parameter sets as ‘light Higgs scenario’. We found in [2] that the allowed parameter region of the light Higgs type disappears for $\tan\beta_0 \gtrsim 10$. As we shall see later, the light Higgs scenario is realized for small $|\kappa|$ and always contain two light bosons.

In contrast to the MSSM, there is the tree-level CP violation in the Higgs sector, characterized by the parameter \mathcal{I} . The CP violation in the Higgs sector of the MSSM is induced by the loop corrections of the squarks and others. For example, $\text{Im}(\mu A_q)$, where A_q is the squark A -term, generates the scalar-pseudoscalar mixing elements in the neutral Higgs mass matrix. This CP violation also affects the neutron EDM, so that the squark mass and/or the relative phase of μ and A_q are constrained not to exceed the upper bound on the EDM. The effect of this CP violation on the Higgs spectrum and gauge couplings have been studied by Carena, et al.[3]. They found that sufficiently large CP violation mixes the scalar and pseudoscalar, so that the lightest Higgs boson has very small gauge coupling to Z boson to escape from the present mass bound. Although one expects strongly first-order EWPT with such a light boson, we found that the CP violation weakens the EWPT, which was strongly first order because of the light stop in the CP-conserving case[4].

On the other hand, the CP violation in the Higgs sector of the NMSSM can escape from the bound due to the EDM[2], while it can generate the CP-violating bubble wall created at the first-order EWPT. We shall see the effect of the tree-level CP violation on the EWPT below.

3 Effective potential

In addition to the tree-level potential (2.4), we include the one-loop corrections coming from the loops of the third generation of quarks and squarks, the gauge bosons and the singlet fermion. The mass-squared matrix of the neutral Higgs bosons and the mass of the charged Higgs boson are defined as the second derivatives of the effective potential evaluated at the vacuum. The explicit forms of these derivatives are given in [2].

The finite-temperature effective potential is given by

$$V_{\text{eff}}(\mathbf{v}; T) = V_0(\mathbf{v}) + \Delta V(\mathbf{v}; T), \quad (3.1)$$

where V_0 is the tree-level Higgs potential (2.4). The one-loop correction is

$$\begin{aligned} \Delta V(\mathbf{v}; T) = & 3 \left[F_0(\bar{m}_Z^2) + \frac{T^4}{2\pi^2} I_B\left(\frac{\bar{m}_Z}{T}\right) + 2F_0(\bar{m}_W^2) + 2 \cdot \frac{T^4}{2\pi^2} I_B\left(\frac{\bar{m}_W}{T}\right) \right] \\ & - 2 \left[F_0(\bar{m}_{\psi_N}^2) + \frac{T^4}{2\pi^2} I_F\left(\frac{\bar{m}_{\psi_N}}{T}\right) \right] \\ & + N_C \sum_{q=t,b} \left\{ 2 \sum_{j=1,2} \left[F_0(\bar{m}_{\tilde{q}_j}^2) + \frac{T^4}{2\pi^2} I_B\left(\frac{\bar{m}_{\tilde{q}_j}}{T}\right) \right] - 4 \left[F_0(\bar{m}_q^2) + \frac{T^4}{2\pi^2} I_F\left(\frac{\bar{m}_q}{T}\right) \right] \right\}, \end{aligned}$$

$$(3.2)$$

where \bar{m} denotes the field-dependent masses, given in Appendix A and

$$F_0(m^2) = \frac{1}{64\pi^2} (m^2)^2 \left(\log \frac{m^2}{M^2} - \frac{3}{2} \right), \quad (3.3)$$

$$I_B(a) = \int_0^\infty dx x^2 \log \left(1 - e^{-\sqrt{x^2+a^2}} \right), \quad (3.4)$$

$$I_F(a) = \int_0^\infty dx x^2 \log \left(1 + e^{-\sqrt{x^2+a^2}} \right). \quad (3.5)$$

Here we adopt the $\overline{\text{DR}}$ scheme with the renormalization scale M , which we determined in such a way that the one-loop correction to the potential vanishes at the vacuum. The order parameters $\mathbf{v} = (v_1, v_2, v_3, v_4, v_5)$ are related to the expectation values of the Higgs fields as follows,

$$(v_1, v_2, v_3, v_4, v_5) = (v_d, v_u \cos \Delta\theta, v_u \sin \Delta\theta, v_n \cos \Delta\varphi, v_n \sin \Delta\varphi), \quad (3.6)$$

where $\Delta\theta = \theta - \theta_0$ and $\Delta\varphi = \varphi - \varphi_0$. Then the tree-level potential is expressed as

$$\begin{aligned} V_0(\mathbf{v}) = & \frac{1}{2}m_1^2 v_1^2 + \frac{1}{2}m_2^2(v_2^2 + v_3^2) + \frac{1}{2}m_N^2(v_4^2 + v_5^2) \\ & - [R_\lambda(v_2 v_4 - v_3 v_5) - I_\lambda(v_3 v_4 + v_2 v_5)] v_1 - \frac{1}{3} [R_\kappa(v_4^2 - 3v_5^2)v_4 - I_\kappa(3v_4^2 - v_5^2)v_5] \\ & + \frac{g_2^2 + g_1^2}{32}(v_1^2 - v_2^2 - v_3^2)^2 + \frac{|\lambda|^2}{4} [(v_1^2 + v_2^2 + v_3^2)(v_4^2 + v_5^2) + v_1^2(v_2^2 + v_3^2)] \\ & + \frac{|\kappa|^2}{4}(v_4^2 + v_5^2)^2 + \frac{v_1}{2} [\mathcal{R}(v_2(v_4^2 - v_5^2) + 2v_3 v_4 v_5) - \mathcal{I}(v_3(v_4^2 - v_5^2) - 2v_2 v_4 v_5)]. \end{aligned} \quad (3.7)$$

The tadpole conditions relieve the one-loop corrections, which modify the expression for the soft masses and the CP-violating parameter I_λ . The results are summarized in Appendix A.

When we examine the consistency of the parameters and study the EWPT, we search for the minimum in the five-dimensional space of the order parameters \mathbf{v} . Noting that the tree-level potential V_0 and all the field-dependent masses are invariant under

$$(v_1, v_2, v_3, v_4, v_5) \mapsto (-v_1, -v_2, -v_3, v_4, v_5), \quad (3.8)$$

the effective potential also has this discrete symmetry. Hence, it is sufficient to search for the minimum in the space with $v_u \geq 0$. This symmetry implies that the first derivatives of the effective potential with respect to v_1, v_2 and v_3 at the origin vanish at any temperature.

The phase transitions are studied by searching for minima of the effective potential at each temperature. Among the phase transitions, the EWPT is defined as the transition at which $v(T) \equiv \sqrt{v_1^2(T) + v_2^2(T) + v_3^2(T)}$ vanishes when temperature is raised, irrespective

of $v_n(T) \equiv \sqrt{v_4^2(T) + v_5^2(T)}$, where $\mathbf{v}(T)$ denotes the absolute minimum of the effective potential at temperature T . For successful electroweak baryogenesis, the EWPT must be strongly first order, in order for the generated baryon number not to be washed out by the sphaleron process. In the MSSM, this requires a light stop, whose mass is less than the top quark mass. Then, the contribution of the light stop to the effective potential, proportional to $T^4 I_B(\bar{m}_{\tilde{t}_1}/T)$, produces an effective Tv^3 -term with a negative coefficient. Although such terms also come from the gauge boson loops, the stop contribution is much larger because of the large Yukawa coupling and the color degrees of freedom[5]. Such a light stop is realized when the singlet stop soft mass almost vanishes, while the doublet soft mass cannot be taken so small at the same time to avoid too large deviation of the ρ -parameter from unity. Hence, a successful baryogenesis in the MSSM requires a specific breaking of supersymmetry.

In the NMSSM, the scalar trilinear term in the tree-level potential is expected to yield strongly first order EWPT[6]. Indeed, the EWPT was studied for a wide range of parameter space and was found to have more chances to be first order for smaller Higgs mass[7]. The naive argument of [6] is as follows: If the EWPT proceeds along the straight line in the order parameter space, connecting the origin and the minimum of the effective potential corresponding to the broken phase, one can parameterize the order parameters as

$$\begin{aligned} v_d &= v \cos \beta(T) = y \cos \alpha(T) \cos \beta(T), \\ v_u &= v \sin \beta(T) = y \cos \alpha(T) \sin \beta(T), \\ v_n &= y \sin \alpha(T), \end{aligned} \tag{3.9}$$

with (almost) constant $\alpha(T)$ and $\beta(T)$ at each temperature T . Then the tree-level potential is written as

$$\begin{aligned} V_0 &= \frac{1}{2} \left((m_1^2 \cos^2 \beta + m_2^2 \sin^2 \beta) \cos^2 \alpha + m_N^2 \sin^2 \alpha \right) y^2 \\ &\quad - \left(R_\lambda \cos^2 \alpha \sin \alpha \cos \beta \sin \beta + \frac{1}{3} R_\kappa \sin^3 \alpha \right) y^3 + \dots \end{aligned} \tag{3.10}$$

For appropriate parameters, the coefficient of the y^3 -term is negative, which makes the phase transition along y -direction strongly first order. In the MSSM, the EWPT proceeds along an almost constant- β line[8]. Since there is no specific symmetry among the doublets and the singlet, the validity of the parametrization (3.9) with a constant α is not obvious. As we shall see below, the phase transitions in the NMSSM are classified into several types, only one of which admits the parameterization of the order parameters in (3.9).

4 Possible phases and transitions

Before presenting the numerical results, we discuss the possible phases and transitions among them. A phase at each temperature is characterized by the location of the minimum

of the effective potential $\mathbf{v}(T)$. Among the components of \mathbf{v} , v and v_n are related to the symmetries of the model. Obviously v is the order parameter of the gauge symmetry, while v_n is the order parameter of a global $U(1)$ symmetry. This is because in the subspace of $v_n = 0$ ($v_4 = v_5 = 0$), the effective potential is invariant under the global $U(1)$ transformation $v_2 + iv_3 \mapsto e^{i\alpha}(v_2 + iv_3)$. We denote the phases of different symmetries as listed in Table 1. For any sensible parameters, the model is in the phase-EW at

phase	order parameters	symmetries
EW	$v \neq 0, v_n \neq 0$	fully broken
I, I'	$v = 0, v_n \neq 0$	local $SU(2)_L \times U(1)_Y$
II	$v \neq 0, v_n = 0$	global $U(1)$
SYM	$v = v_n = 0$	$SU(2)_L \times U(1)_Y$, global $U(1)$

Table 1: Classification of the phases in the NMSSM.

much lower temperatures than the electroweak scale. At sufficiently high temperatures, where all the symmetries are restored, it is in the phase-SYM. In the limit where the singlet fields decouple by $v_n \rightarrow \infty$, the phase-EW at low temperatures transits to the phase-I with almost constant $v_n(T)$, resulting in the MSSM-like EWPT. In the case of $v_{0n} = O(100)\text{GeV}$, all the phases can appear at temperature of the electroweak scale so that various patterns of phase transitions will be found.

The existence of the phases-I and II is a novel feature of the NMSSM. In particular, in the subspace of $v = 0$, the potential can develop a nontrivial minimum for some parameters. To see this fact, we consider the tree-level potential for $v_1 = v_2 = v_3 = 0$,

$$\hat{V}_0(v_n) = V_0(0, 0, 0, v_n \cos \Delta\varphi, v_n \sin \Delta\varphi) = \frac{1}{2}m_N^2 v_n^2 - \frac{1}{3}\hat{R}_\kappa v_n^3 + \frac{|\kappa|^2}{4}v_n^4, \quad (4.1)$$

where $\hat{R}_\kappa = \frac{1}{\sqrt{2}}|\kappa A_\kappa| \cos[\text{Arg}(\kappa A_\kappa) + 3\Delta\varphi]$. When $\hat{R}_\kappa^2 > 4|\kappa|^2 m_N^2$, $\hat{V}_0(v_n)$ has a local minimum at $v_n = \alpha_+ = (\hat{R}_\kappa + \sqrt{\hat{R}_\kappa^2 - 4|\kappa|^2 m_N^2})/(2|\kappa|^2)$, where the potential is

$$\hat{V}_0(\alpha_+) = \frac{\alpha_+^2}{4} \left(m_N^2 - \frac{\hat{R}_\kappa^2 + \hat{R}_\kappa \sqrt{\hat{R}_\kappa^2 - 4|\kappa|^2 m_N^2}}{12|\kappa|^2} \right). \quad (4.2)$$

For a very small $|\kappa|$ with moderate $|A_\kappa|$ and m_N^2 , α_+ is so large that $\hat{V}_0(\alpha_+)$ becomes smaller than the potential at the electroweak vacuum, when the right-hand side of (4.2) is negative. That is, for such a parameter set, the phase at zero temperature is the phase-I. Although we must exclude such a parameter set, some parameters can admit the phase-I of this kind as an intermediate phase at finite temperature. We shall refer to the phase realized for a small $|\kappa|$ as phase-I', in order to distinguish it from the phase-I which occurs as the intermediate phase in the MSSM-like phase transition. Both the phases will appear at finite temperature with the same symmetry property. However, the Higgs spectrum

for the parameters which admits the phase-I' is different from that in the MSSM-like parameters, in that the former contains a light scalar. In the limit $\kappa = 0$, the model is invariant under a phase transformation of N and H_u , which is spontaneously broken by nonzero v_{0n} . This symmetry is explicitly broken by small $|\kappa|$, which results in a light Higgs boson. It should be noted that this argument is not so altered by the radiative corrections. If we set $v_1 = v_2 = v_3 = 0$ in the effective potential, the correction dependent on v_n arises only from the loop of the singlet fermion, whose contribution is negligible for $|\kappa| \ll 1$. This also implies that the value of the effective potential in the phase-I' is almost independent on temperature.

As temperature is lowered, the phase-SYM at high temperature transits to the phase-EW via various phases. We enumerate the four types of transitions which we encounter in the numerical analysis:

$$\begin{array}{ll} \text{A: SYM} \rightarrow \text{I} \Rightarrow \text{EW} & \text{B: SYM} \rightarrow \text{I}' \Rightarrow \text{EW} \\ \text{C: SYM} \Rightarrow \text{II} \rightarrow \text{EW} & \text{D: SYM} \Rightarrow \text{EW} \end{array}$$

Here the double arrow indicates the transition at which the electroweak gauge symmetry is broken. The second transition of type A is the MSSM-like EWPT, which proceeds with almost constant $v_n(T)$. The transition of type D was found to be strongly first order transition in the case of light Higgs boson[6]. We shall see below that such a transition for the parameters consistent with the lower bound on the Higgs mass occurs in the presence of a light stop. The other two-stage transitions are novel in the NMSSM. In principle, there could be a three-stage transition, but it will be realized for very restricted parameters.

5 Numerical results

The behavior of the phase transitions is studied by numerically searching for the minimum of the effective potential (3.1). We do not use the high-temperature expansion to evaluate the integrals (3.5), since there are particles of weak scale mass. The method we employed is the same as that in [4]. We perform the minimum search of the effective potential for various parameter sets. Among the parameters, the common ones are those known from experiments such as $v_0 = 246\text{GeV}$, $m_W = 80.3\text{GeV}$, $m_Z = 91.2\text{GeV}$, $m_t = 175\text{GeV}$, $m_b = 4.2\text{GeV}$, and we adopt the A -parameters in the squark sector $A_t = A_b = 20\text{GeV}$, which are taken not so large that the squark masses-squared do not become negative. As for the squark soft masses, we take the following three cases: in the heavy squark case the doublet soft mass is taken to be $m_{\tilde{q}} = 1000\text{GeV}$ and the singlet ones are $m_{\tilde{t}_R} = m_{\tilde{b}_R} = 800\text{GeV}$. In the light squark case-I, $m_{\tilde{q}} = 1000\text{GeV}$ and $m_{\tilde{t}_R} = m_{\tilde{b}_R} = 10\text{GeV}$, and in the light squark case-II, $m_{\tilde{q}} = 500\text{GeV}$ and the same singlet soft mass as the case-I. Now the remaining parameters are those characterizing the vacuum $\tan\beta_0$, θ_0 , φ_0 and v_{0n} , and the complex ones, λ , κ , A_λ , A_κ . The soft masses in the Higgs potential can be expressed in terms of the other parameters by use of the tadpole conditions, as shown in Appendix A.

As discussed in Section 3, the independent parameters in the Higgs sector are $|\lambda|$, $|\kappa|$, R_λ , R_κ , \mathcal{R} and \mathcal{I} . We use the charged Higgs mass m_{H^\pm} , instead of R_λ , through the relation

$$m_{H^\pm}^2 = m_W^2 - \frac{1}{2} |\lambda|^2 v_0^2 + \frac{1}{\sin \beta_0 \cos \beta_0} \left[\left(R_\lambda - \frac{1}{2} \mathcal{R} v_{0n} \right) v_{0n} + \left\langle \frac{\partial^2 \Delta V(\mathbf{v}; 0)}{\partial \phi_d^+ \partial \phi_u^-} \right\rangle \right], \quad (5.1)$$

where $\langle \cdots \rangle$ represents the value evaluated at the vacuum. The expression of the second derivative with respect to the charged Higgs field is rather lengthy and almost the same as that in the MSSM, which is given in [4], except for μ -parameter replaced with $\lambda v_{0n} e^{i\varphi_0} / \sqrt{2}$.

We thoroughly examined the parameter space of the model for $v_{0n} = 100 - 1000 \text{ GeV}$ in the absence of CP violation[2]. The allowed parameter sets are defined to satisfy the two conditions; i) the Higgs bosons whose coupling to the Z boson is larger than a tenth of that in the standard model Higgs boson be heavier than 114 GeV (the spectrum condition), and ii) the prescribed vacuum be the absolute minimum of the effective potential (the vacuum condition). The second condition also requires that all the masses-squared of the scalars in the model be positive, including the squarks and sleptons. The allowed regions in the parameter space are roughly classified into two groups; one contains a light Higgs boson with small coupling to the Z boson, and the other is similar to the MSSM, with the lightest Higgs boson heavier than the present bound. The former exists only when v_{0n} is $O(100) \text{ GeV}$, and within the region, $|\kappa| \lesssim 0.1$. The latter region always exists for a large $|\kappa|$ regime when v_{0n} is small, and extends to small $|\kappa|$ regime as v_{0n} grows to reach the MSSM limit. In the following, we show the results on the phase transitions for several points within the allowed regions for $v_{0n} = 200 \text{ GeV}$, $\tan \beta_0 = 5$ and $A_\kappa = -100 \text{ GeV}$, to illustrate the four types of the transitions discussed in the previous section in the absence of CP violation. For $m_{H^\pm} = 600 \text{ GeV}$ in the heavy squark case, the allowed region in the (λ, κ) -plane is shown as a white region in Fig. 1, where the grey region is excluded by the spectrum condition and the black region is excluded by the vacuum condition[2]. Later, we introduce the explicit CP violation in the Higgs sector which does not induce the neutron EDM and examine its effects on the phase transitions.

5.1 CP-conserving case

We take all the parameters to be real and set $\theta_0 = \varphi_0 = 0$. For $v_{0n} = 200 \text{ GeV}$, $\tan \beta_0 = 5$ and $A_\kappa = -100 \text{ GeV}$, we can find all the four types of phase transitions by choosing an appropriate set of m_{H^\pm} , λ , κ and the squark soft masses. The transition of type D is observed only with the light squark cases in the light Higgs scenario. The transition of type A is found in rather broad region with the heavy Higgs boson, but a light stop is necessary for the EWPT to be strongly first order just as in the case of the MSSM. The transitions of type B and C appear in the light Higgs scenario at $|\kappa| \ll 1$. The type-C transition also requires a light stop to be strongly first order. Here we take $(\lambda, \kappa) = (0.9, -0.9)$ and $(0.82, -0.05)$ with $m_{H^\pm} = 600 \text{ GeV}$ in the light squark-I case. Each corresponds to the transition of type A and C, respectively. An example of the

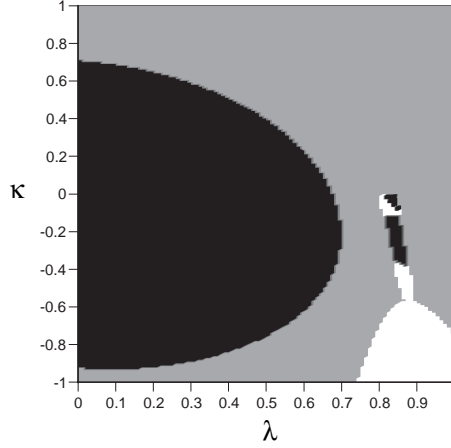


Figure 1: The allowed region in the (λ, κ) -plane for $v_{0n} = 200\text{GeV}$, $\tan\beta_0 = 5$, $A_\kappa = -100\text{GeV}$ and $m_{H^\pm} = 600\text{GeV}$ in the heavy squark case.

type-B transition, we choose $(\lambda, \kappa) = (0.85, -0.1)$ with $m_{H^\pm} = 600\text{GeV}$ in the heavy squark case. For an example of the type-D transition, we adopt $(\lambda, \kappa) = (0.96, -0.02)$ and $m_{H^\pm} = 700\text{GeV}$ in the case of the light squark-II. We shall refer to each parameter set as A, C, B, and D, respectively. The masses and g_{HZZ}^2 of the mass eigenstates are listed in Table 2 for each parameter set. Here g_{HZZ} is the couplings to the Z boson normalized by that of the standard model. For these parameter sets, the only one CP-even scalar has

		H_1	H_2	H_3	H_4	H_5
A	$m_{H_i}(\text{GeV})$	119.53	203.59	265.74	617.24	637.47
	$g_{H_iZZ}^2$	0.9992	5.926×10^{-4}	0	0	1.884×10^{-4}
B	$m_{H_i}(\text{GeV})$	38.89	75.31	131.11	625.61	627.95
	$g_{H_iZZ}^2$	6.213×10^{-8}	0	0.9999	6.816×10^{-5}	0
C	$m_{H_i}(\text{GeV})$	42.24	63.49	117.25	625.09	627.44
	$g_{H_iZZ}^2$	0.00188	0	0.9980	9.541×10^{-5}	0
D	$m_{H_i}(\text{GeV})$	41.88	58.62.08	115.15	730.51	734.58
	$g_{H_iZZ}^2$	0	1.015×10^{-4}	0.9997	1.632×10^{-4}	0

Table 2: The mass and g_{HZZ}^2 of the Higgs mass eigenstates for the four parameter sets.

the coupling almost equal to unity, while the others have almost zero. This is a general feature when the charged scalar is rather heavy, since the tree-level mass matrix of the CP-even scalar has an eigenvector near $(\cos\beta_0, \sin\beta_0, 0)$ so that the corresponding mass eigenstate has $g_{HZZ}^2 \simeq 1$ [2]. The mass eigenvalues are also be understood by recalling the properties of the tree-level mass matrices as follows. The mass eigenvalues of the pseudoscalar always satisfy $m_{A_1}^2 < \hat{m}^2 < m_{A_2}^2$, where $\hat{m}^2 = m_{H^\pm}^2 - m_W^2 + |\lambda|^2 v_0^2/2$. When \hat{m}^2 is large, the mass eigenvalues of the CP-even scalars satisfy $m_{S_1}^2 < m_{S_2}^2 < \hat{m}^2 < m_{S_3}^2$. As discussed in the previous section, there is a light pseudoscalar A_1 for small $|\kappa|$ and

$v_{0n} \neq 0$. Then the relations $\text{Tr}\mathcal{M}_S^2 \simeq \hat{m}^2(1 + v_0^2 \sin^2 \beta_0 \cos^2 \beta_0 / v_{0n}^2) + m_Z^2$ and $\text{Tr}\mathcal{M}_P^2 \simeq \hat{m}^2(1 + v_0^2 \sin^2 \beta_0 \cos^2 \beta_0 / v_{0n}^2)$ imply that $m_{A_2} \simeq m_{S_3} \simeq \hat{m}$, and that m_{S_1} must be smaller than m_Z , once we impose the condition $m_{S_2} > 114\text{GeV}$. Thus the spectrum of the neutral Higgs bosons listed in Table 2 is generic for $|\kappa| \simeq 1$ (set A) and $|\kappa| \ll 1$ (B, C, D), when the charged scalar is heavy. This should be contrasted to the situation in the MSSM, in which the pseudoscalar and the heavier scalar decouple leaving the lighter scalar at the weak scale, in the limit of large m_{H^\pm} .

The phase transitions are studied by searching for the global minimum of the effective potential, which is a function of $(v_1, v_2, v_4) = (v_d, v_u, v_n)$ in the CP-conserving case. Which type of transitions is realized is anticipated from the structure of the zero-temperature potential. To show the potential schematically, we define the reduced effective potential as a function of (v, v_n) , which is a section of the three-dimensional order parameter space with a constant $\tan \beta(T)$ at the minimum,

$$\tilde{V}_{\text{eff}}(v, v_n; T) = V_{\text{eff}}(v \cos \beta(T), v \sin \beta(T), 0, v_n, 0; T) - V_{\text{eff}}(0, 0, 0, 0, 0; T). \quad (5.2)$$

The contour plots of the reduced potential at zero temperature for the parameter sets A–D are shown in Figs. 2 and 3. The left-hand plot in Fig. 2 suggests that the phase

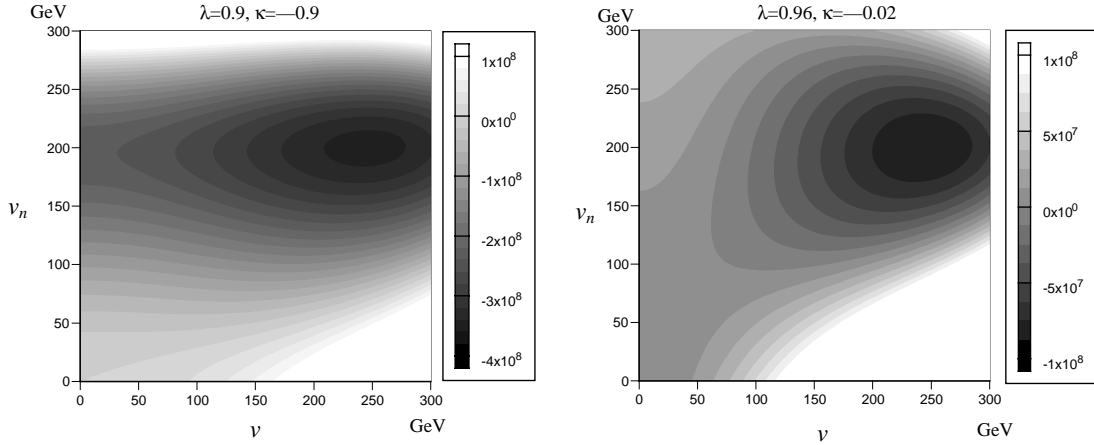


Figure 2: The contour plot of the reduced effective potential at $T = 0$ for the parameter set A (left-hand side) and D (right-hand side).

transition proceeds along almost constant v_n , while the right-hand plot seems to justify the parametrization of (3.9) with a constant $\alpha(T)$. The left-hand plot in Fig. 3 shows there is a local minimum along $v = 0$. As discussed in the previous section, the height of that minimum is almost independent of T , while that at the vacuum grows as temperature is raised, so that the transition will be of the type-B. To show the global structures, we adopt a larger scale for the vertical axes in Fig. 3 than those in Fig. 2. If we used the same scale for them, the contour plot for the set C would look like that for the set D.

To see how the transitions proceed, we show the temperature dependence of the local minima of the effective potential corresponding to the phases, subtracted by the value at

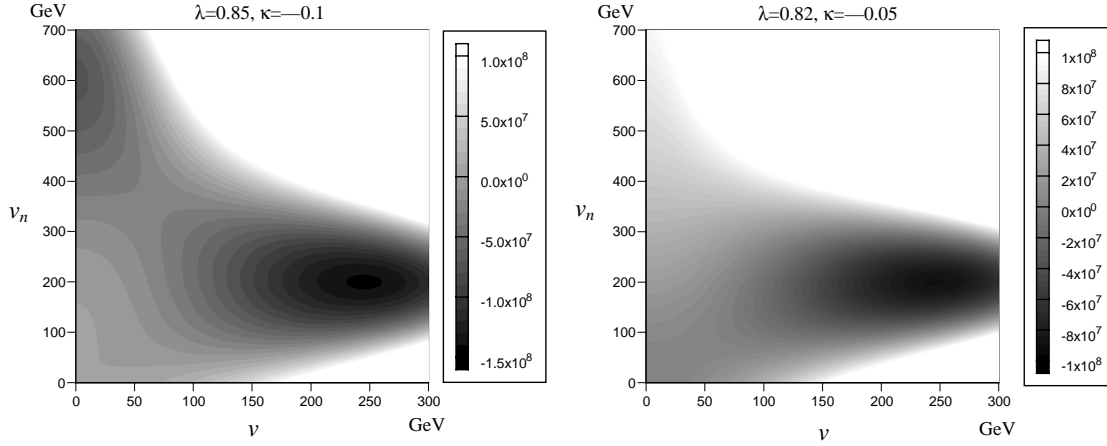


Figure 3: The contour plot of the reduced effective potential at $T = 0$ for the parameter set B (left-hand side) and C (right-hand side).

the origin. In the numerical search for the minima, we found a few distinct convergent points at the same temperature, which are displayed in the plots as different curves. For the set A, the result is plotted in Fig. 4, which shows that the phase-EW changes to the phase-I at $T_C = 120.47\text{GeV}$. There the order parameters change from $(v, v_n) = (106.92\text{GeV}, 194.23\text{GeV})$ to $(0, 192.75\text{GeV})$. This implies the EWPT is first order with

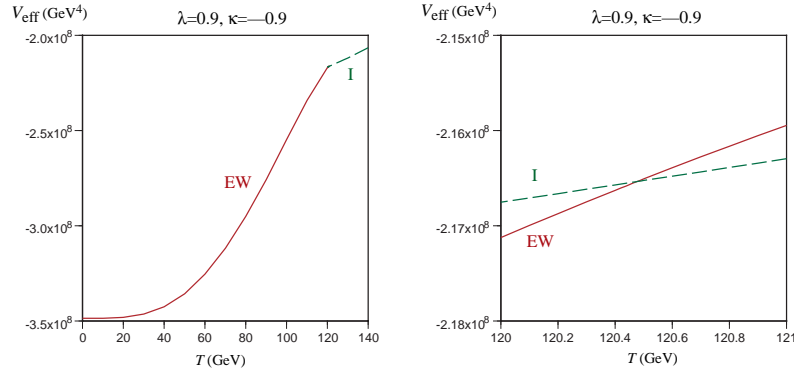


Figure 4: The effective potentials at the local minima corresponding to the phase-EW (solid curve) and the phase-I (dashed curve) for the parameter set A. The right-hand plot is the close view of the left-hand one near the transition temperature.

$v_C/T_C = 0.89$. Although we cannot determine the sphaleron decoupling condition in the NMSSM, since we have not found the sphaleron solution in the model, that will be similar to that in the MSSM for the set A, whose spectrum and phase transition are MSSM-like. Then this parameter will not provide sufficiently strong first-order transition, but the transition will become stronger for a lighter stop, as in the case of the MSSM.

An example for the transition of type B is shown in Fig. 5. At $T_C = 110.26\text{GeV}$, the low-temperature phase-EW transits to the phase-I', which gives its place to the phase-

SYM at $T > 500\text{GeV}$. There the order parameters changes from $(v, v_n) = (208.13\text{GeV}, 248.85\text{GeV})$ to $(0, 599.93\text{GeV})$. This is a very strongly first-order transition with respect to the electroweak order parameter. As discussed in the previous section, the slopes of the curves

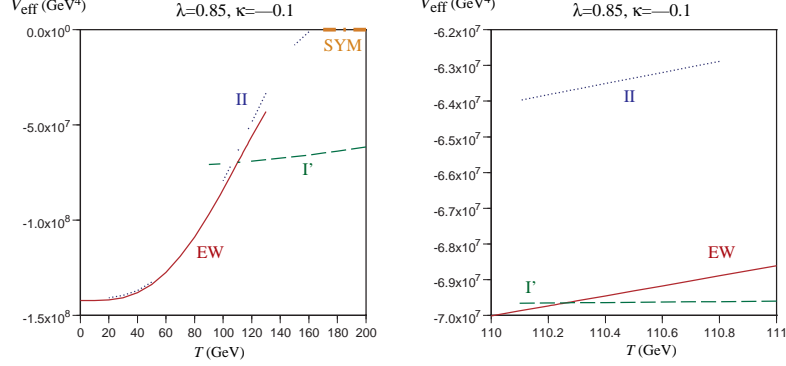


Figure 5: The effective potentials at the local minima corresponding to the phase-EW (solid curve), the phase-I' (dashed curve), the phase-II (dotted curve) and the phase-SYM (thick dotted-dashed curve) for the parameter set B. The right-hand plot is the close view of the left-hand one near the transition temperature.

corresponding to the phase-I and I' are smaller than the others. In particular, the potential at the phase-I' is almost independent of temperature because of small $|\kappa|$.

Fig. 6 illustrates the transition of type C, in which the low-temperature phase-EW changes to the phase-SYM through the intermediate phase-II. At $T_N = 98.76\text{GeV}$, the phase-EW changes to the phase-II, which is converted to the phase-SYM at $T_C = 107.44\text{GeV}$. The order parameters changes from $(v, v_n) = (194.27\text{GeV}, 173.75\text{GeV})$ to $(165.97\text{GeV}, 0)$ at T_N , and from $(109.54, 0)$ to $(0, 0)$ at T_C . The latter is a strongly first-order EWPT.

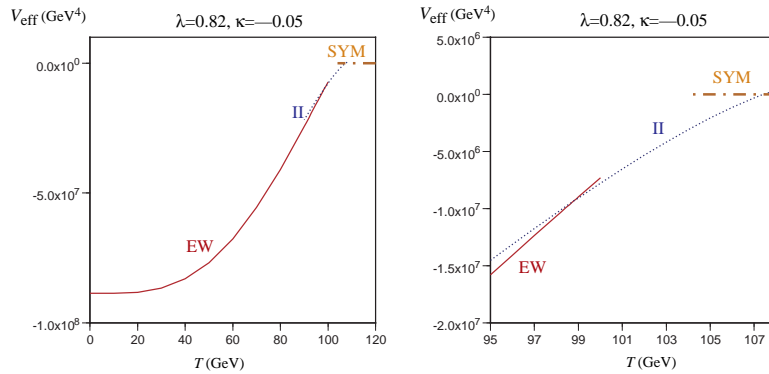


Figure 6: The effective potentials at the local minima corresponding to the phase-EW (solid curve), the phase-II (dotted curve) and the phase-SYM (thick dotted-dashed curve) for the parameter set C. The right-hand plot is the close view of the left-hand one near the transition temperature.

For the parameter set D, the phase transition proceeds as shown in Fig. 7. Only the EWPT occurs at $T_C = 103.14\text{GeV}$ where the order parameter changes from $(v, v_n) =$

(182.49GeV, 192.26GeV) to (0,0). This is a strongly first-order transition first studied in [6]. Although there is also the local minimum corresponding to the phase-II in this case, it does not take part in the phase transition.

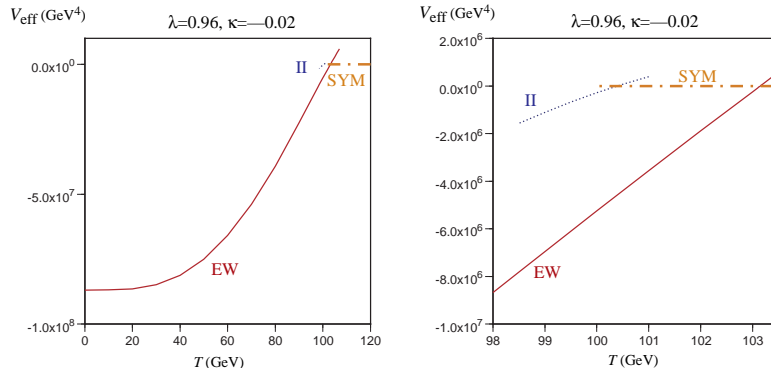


Figure 7: The effective potentials at the local minima corresponding to the phase-EW (solid curve), the phase-II (dotted curve) and the phase-SYM (thick dotted-dashed curve) for the parameter set D. The right-hand plot is the close view of the left-hand one near the transition temperature.

The three parameter sets B, C and D are within the allowed region with light Higgs bosons. What discriminates the types of the transitions are the appearance of the phase-I' and the relative magnitudes of the effective potential at the minima. These factors depend on the parameters in the model. All types of the transitions except for the type-B requires a light stop to admit the strongly first-order EWPT. This is because the term which behaves as Tv^3 with a negative coefficient is effective to make the transition stronger for the three types, while the transition of type-B requires a local minimum along $v = 0$ and proceeds by leaping between the minimum and that corresponding to the phase-EW so that the v^3 -term is not necessary.

5.2 CP-violating case

The phases of the Higgs fields around the phase boundary are important ingredients which determine how much baryon number is generated at the first-order EWPT[1]. We found that the explicit CP violation in the squark sector weakens the v^3 -behavior of the effective potential[4], and expect that the same applies to the transitions which require a light stop. Here we study the effect of CP violation in the tree-level Higgs sector characterized by \mathcal{I} . There are infinite sets of CP violating parameters which yield the same value of \mathcal{I} , so we constrain them in such a way that the phase relevant to the neutron EDM, $\text{Arg}\lambda + \theta_0 + \varphi_0$, vanish¹[2]. In practice, we set $\theta_0 = \varphi_0 = 0$ and take $\text{Arg}\kappa$ as an independent parameter, from which $\text{Arg}A_\kappa$ is determined by the conditions (A.12) and (A.13).

¹The EDM is an odd function of this phase plus the phase of the A -term or the gaugino mass.

Here we concentrate on the effect of the CP violation on the transition for the parameter sets near the set B, for which the EWPT is strongly first order even with heavy stops. For the parameter set B, we introduce the relative phase of κ to $\kappa = -0.1$, δ_κ , and repeat the numerical search for the minima at each temperature. We find that the effective potential at the minimum corresponding to the phase-I' decreases with δ_κ and becomes smaller than that in the phase-EW even at zero temperature for $\delta_\kappa \gtrsim 0.2\pi$. To see this behavior, we adopt another parameter set for which $\lambda = 0.83$ and $\kappa = -0.07$ while the others are the same as the set B, and study temperature dependence of the effective potential at the local minima. The masses and the couplings to the Z boson of the Higgs mass eigenstates are listed in Table 3. Since $|\kappa|$ is not so large, the effect of δ_κ on the mixing of the CP-eigenstates is also small. The behaviors of the effective potential

δ_κ		H_1	H_2	H_3	H_4	H_5
0	$m_{H_i}(\text{GeV})$	38.89	75.31	131.11	625.61	627.945
	$g_{H_i ZZ}^2$	6.213×10^{-8}	0	0.9999	6.816×10^{-5}	0
0.1π	$m_{H_i}(\text{GeV})$	40.04	73.24	131.20	625.54	627.56
	$g_{H_i ZZ}^2$	2.749×10^{-6}	0.00169	0.9982	6.570×10^{-5}	2.363×10^{-6}
0.2π	$m_{H_i}(\text{GeV})$	43.21	66.95	131.38	625.40	627.85
	$g_{H_i ZZ}^2$	3.133×10^{-5}	0.00531	0.9946	6.132×10^{-5}	6.407×10^{-6}

Table 3: The mass and g_{HZZ}^2 of the Higgs mass eigenstates for $(\lambda, \kappa) = (0.83, -0.07)$ and $\delta_\kappa = 0, 0.1\pi$ and 0.2π .

are shown in Fig. 8. For $\delta_\kappa \gtrsim 0.3\pi$, the zero-temperature vacuum is in the phase-I'. The

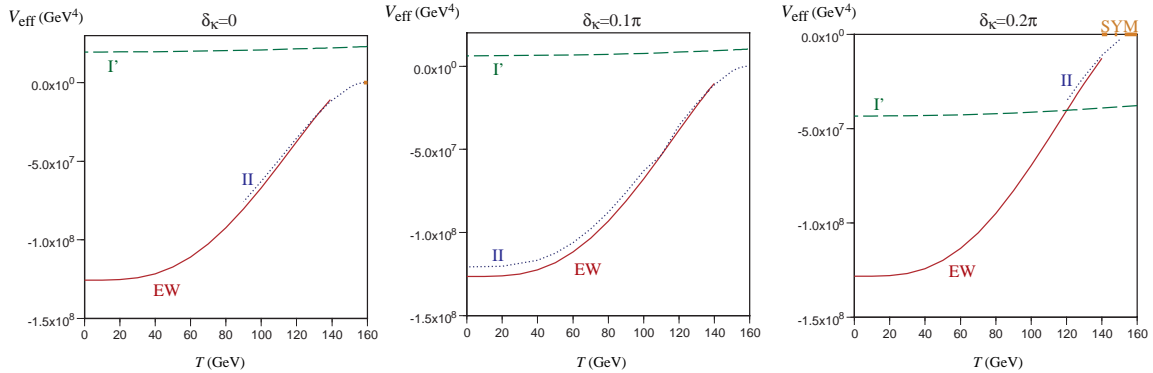


Figure 8: The effective potentials at the local minima corresponding to the phase-EW (solid curve), the phase-I' (dashed curve), the phase-II (dotted curve) and the phase-SYM (thick dotted-dashed curve) for $(\lambda, \kappa) = (0.83, -0.07)$ and $\delta_\kappa = 0, 0.1\pi$ and 0.2π .

transitions for $\delta_\kappa = 0$ and 0.1π are of type C, while that for $\delta_\kappa = 0.2\pi$ is of type B. At the transition temperatures, the order parameters changes as follows:

$$\delta_\kappa = 0; \quad \text{at } T_N = 133.22\text{GeV}, \quad (v, v_n) = (180.74\text{GeV}, 195.49\text{GeV}) \rightarrow (163.16\text{GeV}, 0)$$

$$\begin{aligned}
& \text{at } T_C = 158.27\text{GeV}, \quad (v, v_n) = (26.33\text{GeV}, 0) \rightarrow (0, 0) \\
\delta_\kappa = 0.1\pi; & \text{ at } T_N = 136.58\text{GeV}, \quad (v, v_n) = (173.99\text{GeV}, 195.88\text{GeV}) \rightarrow (154.78\text{GeV}, 0) \\
& \text{at } T_C = 158.27\text{GeV}, \quad (v, v_n) = (26.33\text{GeV}, 0) \rightarrow (0, 0) \\
\delta_\kappa = 0.2\pi; & \text{ at } T_C = 120.16\text{GeV}, \quad (v, v_n) = (200.62\text{GeV}, 208.93\text{GeV}) \rightarrow (0, 750.93\text{GeV})
\end{aligned}$$

The EWPT of the type B for $\delta_\kappa = 0.2\pi$ is strongly first order as that for the parameter set B. This behavior of the potential at the minimum in the phase-I' can be understood as follows. As discussed in the previous section, the potential in this phase can be approximated by the tree-level potential, which is given by (4.2), even at finite temperatures. In that expression, both \hat{R}_κ and m_N^2 are decreasing functions of $\delta_\kappa \leq \pi/2$, and $\hat{V}_0(\alpha_+)$ decreases with δ_κ^2 .

The phase difference relevant to the baryogenesis is that at the phase transition after which the sphaleron process decouples. We have considered such a transition to be the EWPT at which $v(T)$ acquires a nonzero value. Even if the EWPT is strong enough to suppress the sphaleron process after that, no baryon number can be generated at T_C for the transition of type C. As we discussed in the previous section, there is the global $U(1)$ symmetry in the phase-II, so that the phase of $v_2(T) + iv_3(T)$ is undetermined even in the presence of the explicit CP violation. In fact, we observed many degenerate local minima with the same $|v_2(T) + iv_3(T)|$ but with different phases in the minimal search. This implies that the bubble with different phases of the Higgs doublets are randomly created at the EWPT. No net baryon number is generated, if such bubbles of a macroscopic number are created as suggested by a naive argument of the transition[9]. If $v(T)$ at T_C is too small to suppress the sphaleron process, just as in the case of $\delta_\kappa = 0$ and 0.1π above, one may think that the second transition at T_N will be another chance for the baryogenesis. The same argument, however, applies to this case, so that the relative phase of the doublet, as well as that of the singlet, between the two phases are undetermined. Thus the transition of type C is not adequate for the baryogenesis. On the other hand, the phase of the singlet is determined in the phase-I' in the transitions of type B, since the symmetry under phase rotation of the singlet field in the subspace of $v_1 = v_2 = v_3 = 0$ is explicitly broken by the R_κ -term in the tree-level potential. In the example of the transition for $\delta_\kappa = 0.2\pi$ above, the $\varphi(T)$ changes from 0.0492 (phase-EW) to 0.2154 (phase-I'). Further the phase $\varphi(T)$ in the phase-I' is independent of temperature, since all the field-dependent masses are independent of $\varphi = \tan^{-1}(v_5/v_4)$ in this phase, so that no φ -dependent terms are generated at finite temperatures.

²Note that m_N^2 is given by (A.10), while we fixed $|\kappa|$, $|\lambda|$ and the charged Higgs mass, from which R_λ is determined.

6 Discussions

We studied various phase transitions in the NMSSM, characterized by the order parameters $v(T)$ and $v_n(T)$, for the parameters consistent with the lower bound on the Higgs boson, when the expectation value of the singlet scalar takes the value of the weak scale. The phase transitions are classified into four types, one of which is the MSSM-like one, and the others are peculiar to the NMSSM. These novel three types of transitions are realized within the allowed region with a light Higgs boson. One of them is the transition studied in [6], but the other two types are equally possible. We found that the transition of type B can be strongly first order without need of a light stop. For the parameter sets with this type of phase transitions, the Higgs bosons which is expected to be observed in future experiments is heavier than the present mass bound and has almost the same coupling to the Z boson as the Higgs boson in the standard model. Although the two light Higgs boson have very small couplings to the Z boson, their Yukawa couplings to the b quark are the same order as the standard model Higgs boson, so that they may be observed in hadron collider experiments. In order to obtain the sphaleron decoupling condition, one must know the sphaleron solution and its energy for the boundary conditions corresponding to the relevant phase transition. A work in this direction is in progress and the result will be published elsewhere[10]. The results suggest that the sphaleron does exist and its energy is a bit smaller than the original sphaleron in the standard model[11], because of the negative cubic terms in the potential.

We also investigated the effect of the tree-level CP violation on the phase transitions of type B and C. Because of the global symmetry in the intermediate phase-II, the model which exhibits the transition of type C is not suited for the baryogenesis. On the other hand, the difference of $\varphi(T)$ above and below the transition temperature can be large without affecting the neutron EDM. This phase becomes dependent on the spatial coordinate near the bubble wall created at the first-order transition. Noting that the μ -parameter in the MSSM is effectively induced as $\mu = \lambda v_n e^{i\varphi}/\sqrt{2}$, this introduces a new source of space-dependent phase into the mass matrix of the charginos, neutralinos, squarks and sleptons, which will produce new contributions to the source of the baryon number in the supersymmetric standard models[12].

In this work, we have been focused on the static properties of the phase transitions. To evaluate the generated baryon number, we must know about their dynamics. Although the study of the dynamical aspects of the transitions is beyond the scope of this work, we expect that as long as all the mass parameters in the Higgs potential are of the order of the weak scale, the dynamics is not so far from those in the standard model or the MSSM. In fact, we have not encountered an extremely deep minimum or high barrier between the minima of the effective potential in the numerical studies, which may delay the transition or eternally trap the model within an unphysical state. This situation might be altered, if we consider the case of larger v_{0n} but not so large as in the MSSM limit. It will be interesting to investigate the phase diagram of the model for broader range of the

parameters.

Acknowledgements

The authors gratefully thank A. Kakuto and S. Otsuki for valuable discussions. This work was supported by the kakenhi of the MEXT, Japan, No. 13135222.

A Notations

A.1 field-dependent masses

Here we summarize the field-dependent masses \bar{m} used to define the effective potential in terms of the vector \mathbf{v} defined by (3.6). Those of the standard model particles are written by the components in the doublets as

$$\bar{m}_Z^2 = \frac{g_2^2 + g_1^2}{4}(v_1^2 + v_2^2 + v_3^2), \quad \bar{m}_W^2 = \frac{g_2^2}{4}(v_1^2 + v_2^2 + v_3^2), \quad (\text{A.1})$$

$$\bar{m}_t^2 = \frac{|y_t|^2}{2}(v_2^2 + v_3^2), \quad \bar{m}_b^2 = \frac{|y_b|^2}{2}v_1^2. \quad (\text{A.2})$$

The those of the squarks and the singlet fermion depends on the singlet component (v_4, v_5) and are given by

$$\begin{aligned} \bar{m}_{\tilde{t}_{1,2}}^2 &= \frac{m_{\tilde{q}}^2 + m_{\tilde{t}_R}^2}{2} + \frac{g_2^2 + g_1^2}{16}(v_1^2 - v_2^2 - v_3^2) + \frac{|y_t|^2}{2}(v_2^2 + v_3^2) \\ &\quad \pm \frac{1}{2} \left[\left(m_{\tilde{q}}^2 - m_{\tilde{t}_R}^2 + \frac{x_t}{2}(v_1^2 - v_2^2 - v_3^2) \right)^2 \right. \\ &\quad \left. + 2|y_t|^2 \left(\frac{|\lambda|^2}{2}v_1^2(v_4^2 + v_5^2) + |A_t|^2(v_2^2 + v_3^2) - 2[R_t(v_2v_4 - v_3v_5) - I_t(v_3v_4 + v_2v_5)]v_1 \right) \right]^{1/2}, \end{aligned} \quad (\text{A.3})$$

$$\begin{aligned} \bar{m}_{\tilde{b}_{1,2}}^2 &= \frac{m_{\tilde{q}}^2 + m_{\tilde{b}_R}^2}{2} - \frac{g_2^2 + g_1^2}{16}(v_1^2 - v_2^2 - v_3^2) + \frac{|y_b|^2}{2}v_1^2 \\ &\quad \pm \frac{1}{2} \left[\left(m_{\tilde{q}}^2 - m_{\tilde{t}_R}^2 + \frac{x_b}{2}(v_1^2 - v_2^2 - v_3^2) \right)^2 \right. \\ &\quad \left. + 2|y_b|^2 \left(\frac{|\lambda|^2}{2}(v_2^2 + v_3^2)(v_4^2 + v_5^2) + |A_b|^2v_1^2 - 2[R_b(v_2v_4 - v_3v_5) - I_b(v_3v_4 + v_2v_5)]v_1 \right) \right]^{1/2}, \end{aligned} \quad (\text{A.4})$$

$$\bar{m}_{\psi_N}^2 = 2|\kappa|^2(v_4^2 + v_5^2), \quad (\text{A.5})$$

where

$$x_t = \frac{1}{4} \left(g_2^2 - \frac{5}{3}g_1^2 \right), \quad x_b = -\frac{1}{4} \left(g_2^2 - \frac{1}{3}g_1^2 \right), \quad (\text{A.6})$$

$$R_q = \frac{1}{\sqrt{2}} \text{Re} \left(\lambda A_q e^{i(\theta_0 + \varphi_0)} \right), \quad I_q = \frac{1}{\sqrt{2}} \text{Im} \left(\lambda A_q e^{i(\theta_0 + \varphi_0)} \right), \quad (q = t, b). \quad (\text{A.7})$$

As for the convention for the squark sector, refer to [4].

A.2 one-loop tadpole conditions

The mass parameters in the tree-level potential is written in terms of the others by requiring that the first derivatives of the zero-temperature effective potential evaluated at the vacuum be vanish. We call these conditions as the tadpole conditions. The three conditions derived from the derivatives with respect to the CP-even fields are used to express m_1^2 , m_2^2 and m_N^2 as

$$\begin{aligned}
m_1^2 = & \left(R_\lambda - \frac{1}{2} \mathcal{R} v_{0n} \right) v_{0n} \tan \beta_0 - \frac{1}{2} m_Z^2 \cos(2\beta_0) - \frac{|\lambda|^2}{2} (v_{0n}^2 + v_{0u}^2) \\
& - \frac{N_C}{16\pi^2} \left[\frac{g_2^2 + g_1^2}{8} f_+ (m_{\tilde{t}_1}^2, m_{\tilde{t}_2}^2) + \frac{t_1}{2v_{0d}\Delta m_{\tilde{t}}^2} f_- (m_{\tilde{t}_1}^2, m_{\tilde{t}_2}^2) + \left(|y_b|^2 - \frac{g_2^2 + g_1^2}{8} \right) f_+ (m_{\tilde{b}_1}^2, m_{\tilde{b}_2}^2) \right. \\
& \quad \left. + \frac{b_1}{2v_{0d}\Delta m_{\tilde{b}}^2} f_- (m_{\tilde{b}_1}^2, m_{\tilde{b}_2}^2) - 2|y_b|^2 m_b^2 \left(\log \frac{m_b^2}{M^2} - 1 \right) \right] \\
& - \frac{3}{32\pi^2} \left[\frac{g_2^2 + g_1^2}{2} m_Z^2 \left(\log \frac{m_Z^2}{M^2} - 1 \right) + 2 \cdot \frac{g_2^2}{2} m_W^2 \left(\log \frac{m_W^2}{M^2} - 1 \right) \right], \tag{A.8}
\end{aligned}$$

$$\begin{aligned}
m_2^2 = & \left(R_\lambda - \frac{1}{2} \mathcal{R} v_{0n} \right) v_{0n} \cot \beta_0 + \frac{1}{2} m_Z^2 \cos(2\beta_0) - \frac{|\lambda|^2}{2} (v_{0n}^2 + v_{0d}^2) \\
& - \frac{N_C}{16\pi^2} \left[\left(|y_t|^2 - \frac{g_2^2 + g_1^2}{8} \right) f_+ (m_{\tilde{t}_1}^2, m_{\tilde{t}_2}^2) + \frac{t_2}{2v_{0u}\Delta m_{\tilde{t}}^2} f_- (m_{\tilde{t}_1}^2, m_{\tilde{t}_2}^2) \right. \\
& \quad \left. + \frac{g_2^2 + g_1^2}{8} f_+ (m_{\tilde{b}_1}^2, m_{\tilde{b}_2}^2) + \frac{b_2}{2v_{0u}\Delta m_{\tilde{b}}^2} f_- (m_{\tilde{b}_1}^2, m_{\tilde{b}_2}^2) - 2|y_t|^2 m_b^2 \left(\log \frac{m_t^2}{M^2} - 1 \right) \right] \\
& - \frac{3}{32\pi^2} \left[\frac{g_2^2 + g_1^2}{2} m_Z^2 \left(\log \frac{m_Z^2}{M^2} - 1 \right) + 2 \cdot \frac{g_2^2}{2} m_W^2 \left(\log \frac{m_W^2}{M^2} - 1 \right) \right], \tag{A.9}
\end{aligned}$$

$$\begin{aligned}
m_N^2 = & (R_\lambda - \mathcal{R} v_{0n}) \frac{v_{0d} v_{0u}}{v_{0n}} + R_\kappa v_{0n} - \frac{|\lambda|^2}{2} (v_{0d}^2 + v_{0u}^2) - |\kappa|^2 v_{0n}^2 \\
& - \frac{N_C}{16\pi^2 v_{0n}} \left[\frac{t_3}{2\Delta m_{\tilde{t}}^2} f_- (m_{\tilde{t}_1}^2, m_{\tilde{t}_2}^2) + \frac{b_3}{2\Delta m_{\tilde{b}}^2} f_- (m_{\tilde{b}_1}^2, m_{\tilde{b}_2}^2) \right] \\
& + \frac{|\kappa|^2}{4\pi^2} m_{\psi_N}^2 \left(\log \frac{m_{\psi_N}^2}{M^2} - 1 \right). \tag{A.10}
\end{aligned}$$

$$\tag{A.11}$$

The first derivatives with respect to the CP-odd fields lead to the relation among the CP-violating parameters as

$$I_\lambda = \frac{1}{2} \mathcal{I} v_{0n} - \frac{N_C}{16\pi^2} \left[\frac{|y_t|^2 I_t}{\Delta m_{\tilde{t}}^2} f_- (m_{\tilde{t}_1}^2, m_{\tilde{t}_2}^2) + \frac{|y_b|^2 I_b}{\Delta m_{\tilde{b}}^2} f_- (m_{\tilde{b}_1}^2, m_{\tilde{b}_2}^2) \right], \tag{A.12}$$

$$I_\kappa = -\frac{3}{2} \mathcal{I} \frac{v_{0d} v_{0u}}{v_{0n}}. \tag{A.13}$$

Here t_i and b_i are the components of the vector \mathbf{t} and \mathbf{b} defined in [2], respectively, and

$$f_\pm(m_1^2, m_2^2) = m_1^2 \left(\log \frac{m_1^2}{M^2} - 1 \right) \pm m_2^2 \left(\log \frac{m_2^2}{M^2} - 1 \right). \tag{A.14}$$

References

- [1] For a review see, A. Cohen, D. Kaplan and A. Nelson, *Ann. Rev. Nucl. Part. Sci.* **43** (1993) 27.
K. Funakubo, *Prog. Theor. Phys.* **96** (1996) 475.
V. A. Rubakov and M. E. Shaposhnikov, *Phys. Usp.* **39** (1996) 461 (hep-ph/9603208).
- [2] K. Funakubo and S. Tao, hep-ph/0409294.
- [3] M. Carena, J. Ellis, A. Pilaftsis and C. E. M. Wagner, *Nucl. Phys.* **B586** (2000) 92.
- [4] K. Funakubo, S. Tao and F. Toyoda, *Prog. Theor. Phys.* **109** (2003) 415.
- [5] A. Brignole, J. R. Espinosa, M. Quiros and F. Zwirner, *Phys. Lett.* **B324** (1994) 181.
M. Carena, M. Quiros and C. E. M. Wagner, *Phys. Lett.* **B380** (1996) 81.
D. Delepine, J. M. Gerard, R. G. Filipe and J. Weyers, *Phys. Lett.* **B386** (1996) 183.
J. M. Cline and G. D. Moore, *Phys. Rev. Lett.* **81** (1998) 3315.
- [6] M. Pietroni, *Nucl. Phys.* **B402** (1993) 27.
- [7] A. T. Davies, C. D. Froggatt and R. G. Moorhouse, *Phys. Lett.* **372** (1996) 88.
- [8] K. Funakubo, *Prog. Theor. Phys.* **101** (1999) 415.
M. Laine and K. Rummukainen, *Nucl. Phys.* **B597** (2001) 23.
- [9] M. E. Carrington and J. I. Kapsta, *Phys. Rev.* **D47** (1993) 5304.
- [10] K. Funakubo, A. Kakuto, S. Otsuki, S. Tao and F. Toyoda, in preparation.
- [11] F. R. Klinkhammer and N. S. Manton, *Phys. Rev.* **D30** (1984) 2212.
- [12] A. G. Cohen and A. E. Nelson, *Phys. Lett.* **B297** (1992) 111.
P. Huet and A. E. Nelson, *Phys. Rev.* **D53** (1996) 4578.
M. Carena, M. Quirós, A. Riotto, I. Vilja and C. E. M. Wagner, *Nucl. Phys.* **B503** (1997) 387.
M. P. Worah, *Phys. Rev. Lett.* **79** (1997) 3810.
M. Aoki, N. Oshimo and A. Sugamoto, *Prog. Theor. Phys.* **98** (1997) 1179.